Research Square

Preprints are preliminary reports that have not undergone peer review.
They should not be considered conclusive, used to inform clinical practice,
or referenced by the media as validated information.

De novo characterization of AcABI5 transcription factor and physiological responses to salt stress in Alhagi camelorum callus

Zhengtao Yan

1940005621@qq.com

Xinjiang Institute of Ecology and Geography https://orcid.org/0009-0003-1090-2219

Xiangyi Li

Xinjiang Institute of Ecology and Geography

Bo Zhang

Xinjiang Institute of Ecology and Geography

Gangliang Tang

Xinjiang Institute of Ecology and Geography https://orcid.org/0009-0002-1322-7047

Research Article

Keywords: Alhagi camelorum, Callus induction, Salt stress, Antioxidant enzymes, AcABI5, bZIP transcription factor

Posted Date: January 27th, 2026

DOI: https://doi.org/10.21203/rs.3.rs-8449616/v1

License: This work is licensed under a Creative Commons Attribution 4.0 International License.
Read Full License

Abstract

Alhagi camelorum, a dominant leguminous shrub in the saline–hyperarid Taklimakan Desert, can complete its life cycle in salty soils, yet the molecular basis of seedling-stage salt tolerance remains unknown. Here, we developed an in-vitro callus system to dissect this trait without soil heterogeneity. Among 36 hormone regimes, 1.5 mg/L 2,4-D plus 0.5 mg/L 6-BA produced 100 % induction. Exposure of 28-d-old calli to 200 mM NaCl for 48 h caused transient swelling of cortical cells and a 5.3-fold rise in malondialdehyde (MDA). Antioxidant enzymes responded sequentially: superoxide dismutase (SOD) peaked at 6 h to scavenge superoxide, peroxidase (POD) maintained high activity throughout the first 24 h, and catalase (CAT) stabilized after 48 h, jointly keeping H_2O_2 below toxic levels. RNA-seq has identified an up-regulated transcription factor ($log_2FC = 7$) which was a basic leucine-zipper (bZIP) homologue of abscisic acid-insensitive protein 5 (ABI5). Quantitative RT-PCR confirmed 17-fold induction by NaCl and rapid decay after stress removal. Sub-cellular localization of a 35S::GFP-AcABI5 fusion in *Nicotiana benthamiana* epidermis showed exclusive nuclear fluorescence, consistent with a transcriptional regulator. Therefore, our study provides both optimized callus protocols and a candidate gene for engineering salt tolerance in *A. camelorum* and related desert legumes.

Introduction

Soil salinization, exacerbated by climate extremes and land misuse, imposes ionic toxicity and osmotic stress that globally curtail root elongation, biomass allocation, and crop yield potential (van Zelm et al. 2020). Shrinking freshwater reserves now make the reclamation of saline–alkali land a critical imperative for global food security. *Alhagi camelorum* Fisch. (Fig. 1), a deep-rooted perennial legume of Central Asian deserts, forms 40–130 cm thickets of thorny, grey-green shoots that carry obovate leaves and short axillary racemes whose red-purple petals give way to spiralled loment pods (Dong and Zhang 2000; Muhammad et al. 2015; Ullah et al. 2022). *A. camelorum* spans the arid corridor from the Taklimakan to the Iranian Plateau, occurring in northwestern China, Kazakhstan, Afghanistan, Iran, Pakistan, Iraq, Mongolia and India; across these regions it routinely colonizes saline soils with > 200 mM NaCl, making it one of the most salt-tolerant wild legumes (Manafu et al. 2024; Pirasteh-Anosheh et al. 2022; Srivastava et al. 2014).

On the southern rim of the Taklamakan, *A. camelorum* carpets the shifting ecotone between oasis cropland and drifting dunes, forming the keystone thicket that stabilizes soils and defines the desert margin (Tang et al. 2013). A single stand delivers a triple dividend: its thorny lattice brakes the wind and anchors shifting sand, its shoots furnish protein-rich fodder equal to alfalfa, and its resin-rich exudates remain a staple of traditional pharmacopoeias (Kazemi and Ghasemi Bezdi 2021; Muhammad et al. 2014; Zeng et al. 2002), and is also an excellent candidate plant for saline-alkali land remediation (Zheng et al. 2023). Nevertheless, the molecular determinants enabling *A. camelorum* to maintain growth under saline conditions remain largely uncharacterized. Systematic discovery and validation of the underlying salt tolerance genes will provide strategic targets for molecular breeding programs aimed at enhancing crop resilience to soil salinity.

The basic leucine zipper transcription factors (bZIP, TFs) form a highly conserved and functionally diverse transcriptional regulatory family in plants. They are characterized by a conserved bZIP core domain that encompasses a DNA-binding region and a leucine zipper dimerization domain.

Through post-translational modifications, these factors participate in the assembly of multiprotein complexes to regulate downstream gene networks. This family plays a central role in the growth, development, and stress adaptation of leguminous plants (Yue et al. 2023). In stress responses, bZIP TFs exhibit distinct functional specificity and diversity. *GmbZIP60* in soybean (*Glycine max*) can be induced by salt and drought stresses, overexpression of *GmbZIP60* enhances soybean tolerance to salt and drought by directly binding to the promoters of stress-responsive genes (Chai et al. 2025). *GmbZIP19* is a positive regulator of pathogen resistance and a negative regulator to modulate stomatal closure, thereby reducing plant tolerance to salt and drought stresses (He et al. 2020). The nuclear protein GmbZIP110 significantly improves the salt stress adaptability of soybean by binding to the ACGT motif to regulate proline accumulation and Na^+/K^+ homeostasis (Xu et al. 2016). As a dominant sand-fixing plant in arid and semi-arid saline-alkali regions, *A. camelorum* exerts a central role in improving regional soil structure and maintaining ecosystem stability by virtue of its excellent salt and drought tolerance. Therefore, as an important class of transcription factors, it is necessary to investigate the mechanism by which bZIPs regulate salt tolerance-related genes in *A. camelorum.*

In this work, aseptic seedlings of *A. camelorum* served as the experimental material, and young stem explants were subjected to a hormone matrix screen that yielded a single optimized medium supporting rapid, highly synchronous callus proliferation. Exposure of these calli to MS medium supplemented with 200 mM NaCl revealed a temporally orchestrated antioxidant response: early superoxide dismutase (SOD) peak, sustained peroxidase (POD) activity, late catalase (CAT) stabilization and corresponding ion-leakage dynamics, validating the in vitro system as a physiologically relevant salt-stress proxy. Transcriptomic profiling of challenged seedling identified a bZIP TF (Tang et al. 2024), ABI5-homologous, as the most strongly up-regulated regulatory gene; its full-length CDS (1080 bp; 359 amino acids) was cloned and designated *AcABI5*. In-silico analysis predicted a canonical basic leucine-zipper domain and a bipartite nuclear-localization signal (NLS); transient expression of a 35S::GFP-AcABI5 fusion in *Nicotiana benthamiana* confirmed exclusive nuclear accumulation. Quantitative RT-PCR (qRT-PCR) time courses demonstrated a 17-fold induction within 12 h of salt treatment, followed by rapid decay upon stress relief, consistent with a primary transcriptional regulator. These results provide the first functional annotation of a salt-responsive transcription factor in *A. camelorum*, establish a reproducible callus-based transformation platform, and identify *AcABI5* as a candidate gene for molecular breeding of salt-tolerant crops.

Materials and Methods

Material treatment and callus induction

A. camelorum seeds used in this study were collected in July 2023 from the Cele Desert Grassland Ecosystem National Field Scientific Observation and Research Station, Xinjiang Institute of Ecology and Geography, Chinese Academy of Sciences. Mature and plump seeds were vernalized for 48 h, soaked in 75% ethanol for 30 s, and rinsed 3 times with sterile distilled water, followed by immersion in 5% NaOCl for 5 min and washed 5 times with sterile distilled water. The seeds were inoculated on MS medium (Murashige and Skoog 1962) supplemented with 3% (w/v) sucrose and 0.3% (w/v) phytagel (pH = 5.8-6.0), and grown under conditions of 25 ± 1°C, 3000 lx, 16 h light and 8 h dark.

Select aseptic seedlings that are in good growth condition and have a seedling age of approximately 28 days for the callus culture of *A. camelorum*.Young stem segments of approximately 0.5 cm were cut as explants and transferred to culture media containing different concentration combinations of 2,4-dichlorophenoxyacetic acid (2,4-D) and 6-benzylaminopurine (6-BA) for callus induction. The culture conditions were the same as those described previously. To evaluate the growth dynamics of calli, the callus induction rate and relative growth of *A. camelorum* were recorded after 28 days of culture, and the fresh weight of calli was measured using the difference method.The callus induction rate (%), callus growth (g) and relative growth rate (%) were calculated as below:

Callus induction rate (%) = (Number of explants producing calli / Total number of inoculated explants) × 100%

Callus growth (g) = Weight of calli after culture − Weight of calli before culture

Relative growth rate (%) = (Callus growth / Initial fresh weight of calli) × 100%

Determination methods of growth indicators physiological and biochemical indexes

To analyze the physiological status of calli under long-term salt stress, the salt stress treatment group was cultured on callus induction medium (MS medium supplemented with 1.5 mg/L 2,4-D and 0.5 mg/L 6-BA) supplemented with an additional 200 mM NaCl, whereas the control group was maintained on basic callus induction medium without NaCl supplementation.The calli with robust growth and uniform size were transferred to the respective media, with 12 calli per medium and 3 replicates set for each treatment. The culture conditions were as follows: temperature of 25 ± 1°C, 3000 lx, 16 h light and 8 h dark. The fresh weight of calli in both the control and treatment groups was measured, histochemical staining was performed, and the phenotypes of calli were recorded by photography on day 0, day 7, and day 14.

DAB staining and NBT staining: *A. camelorum* calli with uniform size after stress treatment were placed in 50 mL centrifuge tubes. Prepared DAB staining solution and NBT staining solution were added respectively to submerge the calli. Vacuum was slowly applied to 0.8 MPa and maintained for 5 min, then slowly restored to normal pressure. Staining was performed at room temperature in the dark for 12 h. After discarding the staining solution, the calli were rinsed repeatedly with sterile distilled water to

remove residual staining solution. Decolorizing solution was added, and the samples were incubated in a 95°C water bath for 10–30 min until chlorophyll was completely removed.

Evans blue staining: *A. camelorum* calli with uniform size after stress treatment were placed in 50 mL centrifuge tubes. Prepared Evans blue staining solution was added to submerge the calli. Vacuum was slowly applied to 0.8 MPa and maintained for 5 min, then slowly restored to normal pressure. Staining was performed at room temperature in the dark for 6 h. After discarding the staining solution, the calli were rinsed repeatedly with sterile distilled water to remove residual staining solution. Decolorizing solution was added, and the samples were incubated in a boiling water bath for 10–30 min until chlorophyll was completely removed.

DAB solution (1 mg/mL): Weigh out 100 mg of DAB powder and dissolve it in 100 ml of 0.1 mol/L phosphate buffer solution (pH = 7.4) to prepare a 1 mg/mL aqueous solution. Adjust the pH to 3.8 with hydrochloric acid, and store the solution at 4°C in the dark.

NBT solution (0.5 mg/mL): Weigh out 50 mg of NBT powder and dissolve it in 100 mL of 0.1 mol/L phosphate buffer solution (pH = 7.4). Store the solution at 4°C in the dark.

Evans blue solution (0.5 mg/mL): Weigh out 50 mg of Evans blue powder and dissolve it in 100 mL of double-distilled water. After dissolving thoroughly, store the solution at room temperature in the dark.

Decolorizing solution: 95% ethanol, acetic acid, and glycerol were mixed at a volume ratio of 3:1:1 and stored at room temperature in the dark.

To determine the physiological and biochemical indices of *A. camelorum* calli under salt stress, the calli with robust growth and uniform size cultured on the same medium were selected and separately transferred to the media of the salt stress treatment group and the control group. After treatment for 0 h, 6 h, 12 h and 48 h, the calli were snap-frozen in liquid nitrogen and subsequently ground into powder. Crude enzyme extract was prepared to determine the malondialdehyde (MDA) content and antioxidant enzyme activities. Samples were also stored at -80°C for subsequent RNA extraction.

Determination of MDA content and antioxidant enzyme activities: 0.1 g samples were taken from both the control and salt stress treatment groups, with 3 replicates per treatment. Kits purchased from Shanghai Fenxi Biotechnology Co., Ltd. were used to determine the contents of MDA, SOD, POD, and CAT. Detailed instructions are available at http://www.shfxsw.cn.

POD activity unit: One unit (U) of POD activity was defined as a 0.005 change in A_{470} per minute per gram of tissue in each milliliter of reaction system.

SOD activity unit: In the xanthine oxidase-coupled reaction system of the kit, one unit (U) of SOD activity was defined as the amount of enzyme required to achieve a 50% inhibition rate.

CAT activity unit: One unit (U) of CAT activity was defined as the amount of enzyme that catalyzes the degradation of 1 μmol H_2O_2 per minute per gram of tissue.

Total RNA extraction and first-strand cDNA synthesis

Total RNA was extracted from the samples treated in Section 1.5 according to the instructions of the TIANGEN Total RNA Extraction Kit. The concentration and purity of RNA were determined using a Nanodrop, and the integrity of RNA was detected by agarose gel electrophoresis.RNA was reverse-transcribed into cDNA as a template using the TIANGEN FastKing One-Step Genomic DNA Removal and cDNA Synthesis SuperMix according to the instructions.

Screening of candidate genes and analysis of gene expression levels

Based on the research findings of (Tang et al. 2024), we identified 10 candidate genes highly responsive to osmotic stress, namely Asp01G030840, Asp01G035580, Asp02G012850, Asp02G017010, Asp02G034200, Asp04G012530, Asp04G017080, Asp07G002390, Asp07G015930, and Asp08G003230. Using *A. camelorum EF-1α* (Asp06G015730) as the internal reference gene, specific primers were designed using Primer Premier 6.0 (Table S2). cDNA from the control and treatment groups at 6 h as mentioned above was used as the template. qRT-PCR was performed according to the instructions of Vazyme SYBR qRT-PCR Master Mix. The relative expression levels of each gene were calculated using the $2^{-\Delta\Delta Ct}$ method to screen the gene with the highest expression level under salt stress for subsequent experiments.

The gene with the highest expression level was selected for qRT-PCR using cDNA from the control and treatment groups at 0 h, 6 h, 18 h, and 36 h as mentioned above as templates. *A. camelorum EF-1α* and *ACT* (Asp07G013640) were used as internal reference genes. qRT—PCR was performed using Applied Biosystems QuantStudio 1 Real-Time PCR System (Thermo Fisher Scientific, USA), the $2^{-\Delta\Delta Ct}$ method was used to calculate the expression levels of this gene in *A. camelorum* calli at different stress durations (Livak and Schmittgen 2001).

Bioinformatics analysis

The Expasy-ProtParam tool (https://web.expasy.org/protparam/) was used to analyze the physicochemical properties of the predicted Asp07G015930 protein, including molecular weight, theoretical isoelectric point, instability index, aliphatic index, and grand average of hydropathicity. SignalP 6.0 (https://services.healthtech.dtu.dk/services/SignalP-6.0/) was used to predict the signal peptide of the full-length sequence to determine its subcellular localization characteristics.

Homologous sequences of Asp07G015930 were obtained using NCBI Blast (https://blast.ncbi.nlm.nih.gov/Blast.cgi) and Uniprot (https://www.uniprot.org/), and 38 homologous

sequences were screened for subsequent analysis. A phylogenetic tree was constructed using MEGA software, with the Neighbor-Joining method for tree reconstruction, and 1000 bootstrap replicates to evaluate branch support. After construction, the generated phylogenetic tree was optimized and visualized using the online tool ITOL (http://itol.embl.de/).

The protein sequences was submitted to the NCBI-CDD database (https://www.ncbi.nlm.nih.gov/cdd/) to predict conserved domains and identify the bZIP superfamily domain and other related functional domains. The online tool MEME (https://meme-suite.org/meme/tools/meme) was used for conserved motif analysis, with 10 motifs set and a motif length range of 6–50 amino acids. Cis-acting regulatory elements of the promoter were predicted using PlantCARE (https://bioinformatics.psb.ugent.be/webtools/plantcare/html/).TBtools software was used to visualize conserved motifs and generate domain and motif band diagrams(Chen et al. 2023).

The online tool SOPMA program (https://npsa-prabi.ibcp.fr/cgi-bin/npsa_automat.pl?page=/NPSA/npsa_server.html) was used to predict the secondary structure of the protein. The online tool SWISS MODEL (https://swissmodel.expasy.org/) was used to predict the tertiary structure of the protein, generate a 3D structure model based on homology modeling, and evaluate the structure quality. Uniprot and WoLF PSORT (https://wolfpsort.hgc.jp/) were used for subcellular localization prediction.

Subcellular localization

Using SnapGene 6.0.2, specific primers for the *AcABI5* gene were designed based on its CDS sequence, incorporating attB-specific recombination sites of the Invitrogen Gateway® donor vector pDONR-Zeo (Table S3). The gene was cloned using cDNA as mentioned above as the template according to the instructions of Vazyme 2×Phanta Flash Master Mix. The amplified product was detected by 1% agarose gel electrophoresis, and the target fragment was purified by gel extraction and sent for sequencing.

Using pDONR-Zeo as the donor vector, the entry vector was obtained through BP reaction according to the instructions of Invitrogen Gateway™ BP Clonase™ Ⅱ Enzyme Mix and transformed into *Escherichia coli* DH5α competent cells. The cells were cultured on LB solid medium (containing 50 μg/mL Zeocin) at 37°C for 12 h. Single colonies were picked for bacterial liquid PCR identification and sent for sequencing. Plasmids were extracted from correctly sequenced clones for LR reaction.

Using pK7WGF2, a recipient vector containing the enhanced green fluorescent protein (eGFP) reporter gene as the recipient vector, the expression vector was obtained through LR reaction according to the instructions of Invitrogen Gateway® LR Clonase™ Ⅱ Enzyme Mix and transformed into *E. coli* DH5α competent cells. The cells were cultured on LB solid medium (containing 50 μg/mL Spec) at 37°C for 12 h. Single colonies were picked for bacterial liquid PCR identification and sent for sequencing. Plasmids were extracted from correctly sequenced clones for subsequent experiments.

The constructed pK7WGF2-35S::GFP-AcABI5 vector plasmid was transformed into *Agrobacterium* GV3101 and cultured on YEB solid medium (containing 50 μg/mL Spec and 25 μg/mL Rif) at 28°C for 24

h. Correctly sequenced single-colony *Agrobacterium* was expanded and resuspended in an infection solution containing 100 μM Acetosyringone, then incubated statically for 3 h. The empty GFP vector was used as a control and mCherry (NLS) was used as a marker for co-injection into *N. benthamiana* leaves. Observation was performed using a laser confocal microscope after 48 h. Fluorescence was detected with a Zeiss LSM 800 (Carl Zeiss AG, Germany) confocal microscope.

Statistical analysis

IBM SPSS Statistics software (Version 27.0, IBM Corp., Armonk, NY, USA) was used for one-way ANOVA, Duncan's multiple range tests, and Student's *t*-test. Error bars on the graphs indicate the standard deviation of the mean (± SD), calculated from three independent biological replicates ($n = 3$) for each treatment. Data were analyzed, and means with identical letters are considered not significantly different at $P < 0.05$. Asterisks are used to indicate significant differences in Student's *t*-test ($P < 0.05$). GraphPad Prism software was used for plotting graphs (Version 10.1.2, GraphPad Software Inc., San Diego, CA, USA).

Results

Effects of different hormone concentrations on callus induction of A. camelorum

A broad spectrum of auxin–cytokinin regimes (Table S1) evoked callus formation from *A. camelorum* stem explants, yet macroscopic texture, pigmentation and growth kinetics varied markedly (Fig. 2). Sub-threshold concentrations (< 0.2 mg /L 2,4-D; < 0.5 mg /L 6-BA) failed to trigger dedifferentiation, whereas cytokinin dominance (6-BA>2,4-D; groups 4–6, 11–12) canalized tissues toward shoot organogenesis. A positive dose–response relationship between 2,4-D and callus induction rate was evident up to 1.5 mg/L, peaking at a relative growth increment of 110.93 ± 12.52% (group 27). Supra-optimal auxin levels reversed this trend, yielding friable, necrotic tissues. Within the window 1.0–2.0 mg/L 2,4-D and 0.5–1.0 mg/L 6-BA, auxin:cytokinin ratios between 3:1 and 2:1 consistently generated compact, cream-coloured, rapidly proliferating calli. Consequently, the formulation 1.5 mg/L 2,4-D plus 0.5 mg/L 6-BA (group 27) was adopted as the benchmark for all subsequent experimentation.

Determination of physiological and biochemical indexes of A. camelorum calli under salt stress

Exposure to 200 mM NaCl for 14 days imposed a sustained growth arrest on *A. camelorum* calli (Fig. 3A-B). Control and salt-treated tissues exhibited equivalent fresh mass at t_0; thereafter, control calli expanded linearly, retaining a bright-green, nodular morphology, whereas treated calli remained quiescent through day 7 and developed a yellow-green hue. By day 14, mean fresh mass of the stressed population had declined by 15.8% relative to t_0, accompanied by marginal necrosis (Fig. 3A-B), indicating that chronic osmotic stress not only blocked biomass accretion but also drove gradual water loss and cellular decompartmentalization.

Plants rapidly accumulate large amounts of reactive oxygen species (ROS) under stress conditions. The main ROS include hydrogen peroxide (H_2O_2), hydroxyl radicals (•OH), and superoxide anion radicals (O_2^-•) (Juan et al. 2021). Excessive ROS act on unsaturated fatty acids in lipids to form peroxides (such as MDA), causing damage to membrane structure and function, oxidizing DNA bases to induce gene mutations or cell apoptosis (Hossain et al. 2015). POD decomposes H_2O_2 to release oxygen ions, which oxidize DAB to form brown water-insoluble precipitates. The darker the precipitate color, the higher the H_2O_2 content in calli and the more severe the damage. As shown in Fig. 3C, the treatment group showed slight damage on day 7, and H_2O_2 accumulated gradually with time, resulting in more severe damage on day 14. O_2^-•, one of the ROS, can reduce NBT to form blue deposits, thus enabling localization of O_2^-• production sites in calli. The darker the color, the higher the ROS content and the more severe the cell damage. Comparison showed that O_2^-• in the control group mainly accumulated on the side of calli in contact with the medium, and no obvious O_2^-• was observed on the top of calli far from the medium. In the treatment group, obvious O_2^-• accumulation was observed on the top of calli on day 7, and O_2^-• was distributed throughout the calli on day 14, indicating severe ROS damage to the entire calli.

Evans blue is a cell viability dye that stains dead cells light blue but cannot enter living cells. Thus, the darker the staining, the higher the damage degree of calli from the outside to the inside. As shown in Fig. 3C, the control group showed no obvious change after 14 days of treatment, while the cell death degree of the treatment group gradually increased with the extension of stress time. Combined with the results of the three histochemical stainings, we concluded that the regulatory mechanism in *A. camelorum* calli could maintain basic cell survival under moderate to high salt stress for 7 days, but the calli suffered obvious damage after 14 days of continuous salt stress.

Temporal Response Characteristics of the Antioxidant Enzyme System in A. camelorum Calli Under Salt Stress

The enzyme activities and MDA content of *A. camelorum* calli treated with 200 mM NaCl for 0 h, 6 h, 12 h, and 48 h are shown in Fig. 4. As shown in Fig. 4A, compared with the control group, SOD activity began to increase at 6 h after treatment and reached a peak at 12 h, indicating that SOD was activated immediately in the early stage of stress to dismutate O_2^-• into oxygen and H_2O_2, which reflects the ability of plants to scavenge O_2^-• and also leads to H_2O_2 accumulation. SOD activity then decreased to the initial stress level at 48 h.

The activity of POD was similar to that of SOD: it was activated immediately in the early stage of stress and reached a peak at 12 h. Although it decreased at 48 h, there was no significant difference compared with 12 h, and high activity was still maintained (Fig. 4B). The activity of CAT increased significantly at 12 h, while there was no significant difference at other time points compared with the control group, but a downward trend was observed (Fig. 4C).

MDA is a marker product of membrane lipid peroxidation. As shown in Fig. 4D, MDA began to accumulate in calli in the first 12 h of stress but showed no significant increase, indicating that the

antioxidant enzyme system in *A. camelorum* calli effectively scavenged ROS and avoided cell damage. With the extension of stress time, a large amount of MDA accumulated in calli after 48 h of long-term stress, indicating that the scavenging capacity of the antioxidant system in the later stage was insufficient to offset ROS accumulation, leading to aggravated damage to the membrane system of calli.

Screening of candidate genes and determination of their expression levels in calli under salt stress

Specific primers were designed based on the CDS sequences of 10 candidate genes, and qRT-PCR analysis was performed. After salt stress treatment of *A. camelorum* calli, the expression levels of six genes were significantly upregulated, while the expression of two genes (Asp08G003230 and Asp02G034200) exhibited a downregulated trend (Fig. 5A). This may be due to differences in expression regulatory mechanisms between calli (as dedifferentiated non-organs) and organs. Among them, Asp07G015930 showed the highest upregulation (8-fold) and was highly responsive to salt stress. Thus, this gene was selected as the target for subsequent studies.

After 48 h of salt stress treatment, compared with the control group, the average relative expression level of *AcABI5* (Asp07G015930) was upregulated 7-fold at 6 h, reached a maximum of 17-fold at 12 h, and was upregulated 12.9-fold at 48 h (Fig. 5B). This indicates that *AcABI5* is highly responsive to salt stress in *A. camelorum* calli, with its expression level significantly increasing as the stress intensifies. Although there was a slight decrease at 48 h, there was no significant difference compared with 12 h. This suggests that *AcABI5* can rapidly respond to salt stress in *A. camelorum* calli and alleviate the damage caused by salt stress by continuously and highly expressing to regulate downstream genes.

Bioinformatics analysis of AcABI5

Based on transcriptome data (Tang et al. 2024), the CDS length of Asp07G015930 is 1080 bp, encoding 359 amino acids. BLAST analysis using NCBI and UniProtKB databases showed that the protein encoded by this gene has high homology with ABI5 in various plants and has conserved functional domains typical of the bZIP family. Based on its function and sequence characteristics, this gene was named *AcABI5*.

Phylogenetic tree reconstruction was performed using 38 homologous sequences from plants such as *Medicago truncatula* and *Cicer arietinum* obtained by homologous protein alignment of AcABI5. AcABI5 is localized in the Group B branch of the phylogenetic tree and is closely clustered with homologous sequences from species such as *Astragalus alpinus* and *C. arietinum*, forming a legume-specific subclade with high support (Fig. 6A). This branch forms a clear differentiation boundary with multiple *G. max* sequences in Groups C and D, indicating obvious species differentiation of AcABI5 within legumes.

According to the protein domain analysis, the AcABI5 protein possesses a typical bZIP TF domain located in the central region of the protein, consisting of a basic region with the conserved motif N-X7-

R/K and a leucine zipper region with the conserved motif L-X6-L (Figs. 6B and S1). This domain serves as the core functional region determining DNA binding and dimerization.A small number of COG2433 and Men1-related motifs are embedded at both ends, which are highly consistent with other legume homologous proteins. The presence of the bZIP domain indicates that this protein may bind to cis-acting elements to regulate the transcription of downstream genes and play a key role in plant stress responses (such as drought and salinity). Compared with sequences in Group D that contain additional extended domains such as cc_RasGRP1_C or bZIP_plant_BZIP46, AcABI5 maintains a relatively streamlined domain architecture, suggesting that its function is biased towards basic transcriptional regulation rather than multi-motif signal integration. The order of conserved motifs is basically consistent with that of homologous sequences, with no significant deletions or insertions, indicating that the DNA binding and dimerization mechanisms of this protein are highly conserved. In addition, PlantCARE prediction results showed that the promoter of AcABI5 contains the abscisic acid-responsive element (ABRE, i.e., the cis-acting element involved in abscisic acid responsiveness), MYB binding sites involved in drought inducibility, as well as hormone-responsive elements and transcription factor binding sites, among other functional elements (Fig. S2). These elements suggest that the expression of AcABI5 may be regulated by abiotic stresses such as salt stress, thereby providing a basis for its involvement in the transcriptional regulation of salt stress responses.

Secondary structure prediction showed that AcABI5 is mainly composed of random coils (60.45%), with α-helix accounting for 37.88%, β-sheet and β-turn accounting for only 1.11% and 0.56%, respectively, which is consistent with the typical long helix-coil-helix structure of bZIP TFs (Fig. S3B). The linear structure diagram reveals alternating helix/random coil segments at the N-terminus and C-terminus, with a continuous α-helix in the middle, which is a potential DNA binding and dimerization region (Fig. S3B). The tertiary structure model further shows an extended helix spanning the main body of the protein, accompanied by several flexible loops and secondary helix bundles, indicating that the protein may form a stable dimer through helix bundles during DNA binding (Fig. S3C). The synchronous fluctuation of helix and coil probabilities in the curve prediction diagram also supports its ability to undergo regulated conformational changes.

ProtParam analysis showed (Table S4) that AcABI5 is a basic protein consisting of 359 amino acids, with a molecular weight of approximately 40.21 kDa and a theoretical isoelectric point of 9.51. An instability index of 56.46 indicates certain instability in vitro, and an aliphatic index of 66.57 indicates moderate thermal stability at higher temperatures. A grand average of hydropathicity (GRAVY) of − 0.845 indicates that the protein has significant hydrophilicity and is more likely to be located in the nucleus or cytoplasm rather than membranous compartments. SignalP 6.0 predicted no signal peptide in the full-length sequence and classified it as "OTHER", supporting the speculation that it is a nuclear-localized TF, which is consistent with the predictions of Uniprot and WoLF PSORT (Fig. S3A).

Results of bioinformatics analysis indicated that AcABI5 is a member of the bZIP superfamily with typical bZIP transcription factor characteristics: hydrophilic, no signal peptide, and mainly composed of helix structures. It maintains a close evolutionary relationship with multiple forage and legume

homologous proteins in legumes and has a highly consistent domain composition with multi-copy sequences. These results suggest that ABI5 in *A. camelorum* may undertake a conserved transcriptional regulatory function and be closely related to the regulatory network of legumes adapting to drought, salinity, and other stresses.

Subcellular localization

PCR amplified the *AcABI5* full-length CDS (1138 bp) from *A. camelorum* cDNA; electrophoresis and sequencing confirmed its validity (Fig. S4A). Purified products underwent BP recombination with pDONR-Zeo and *E. coli* transformation, and bacterial PCR/sequencing verified entry vector construction for plasmid extraction (Fig. S4C). Subsequent LR recombination between *AcABI5*-pDONR and pK7WGF2, plus *E. coli* transformation, was validated by colony PCR/sequencing, with positive plasmids extracted and preserved (Fig. S4B).The constructed vector was transiently expressed in the leaves of *N. benthamiana*.

As shown in Fig. 7, green fluorescence of 35S::GFP was detected throughout the cells, while green fluorescence was only detected in the nucleus of cells transfected with the fusion vector 35S::GFP-AcABI5. Moreover, the green fluorescence overlapped with the red fluorescence of 35S::mCherry, indicating that the AcABI5 protein is localized in the nucleus and is a typical transcription factor.

Discussion

2,4-D and 6-BA are two commonly used plant growth regulators. 2,4-D is an auxin-like regulator that promotes callus growth at low concentrations and inhibits differentiation at high concentrations. 6-BA is a cytokinin-like regulator that can induce callus differentiation into buds. This experiment comprehensively analyzed the effects of different concentrations of the two hormones on *A. camelorum* callus formation through a full-factorial experiment with concentrations ranging from 0 to 2 mg/L. The results showed that the combination of 1.5 mg/L 2,4-D and 0.5 mg/L 6-BA was the optimal hormone ratio for *A. camelorum* callus proliferation.

Bu et al. (2000) reported that MS medium containing 1.5–2.0 mg/L 2,4-D and 0.5–1.0 mg/L 6-BA was the optimal medium for inducing callus formation and subculture of *A. camelorum* hypocotyl segments. When 2,4-D and 6-BA reach a specific balance, calli of *Alhagi graecorum* form somatic embryos through somatic embryogenesis, which further develop into regenerated plants. When cytokinin is dominant (e.g., high concentration of 6-BA), explants dedifferentiate to form calli and then differentiate into adventitious buds through organogenesis (Hassanein 2004). These results are consistent with those of this experiment. In evaluating the callus induction effect of *A. camelorum*, compared with the traditional qualitative judgment of callus induction efficiency using callus induction rate, callus status, and growth rate (Bu et al. 2000), this experiment also quantitatively compared the induction effects of different groups by determining the relative growth rate of calli, providing a new reference index.

Changes in fresh weight, phenotype, antioxidant enzyme activity, ROS accumulation, MDA accumulation, and cell mortality of calli are comprehensive and intuitive manifestations of callus response to salt stress. This study investigated the responses of the above physiological and biochemical indexes of *A. camelorum* calli at different time points under high salt stress.

Song (2019) reported that salt stress treatment of *Zoysia matrella* calli showed that callus growth was inhibited when NaCl concentration was ≥ 0.6% (approximately 100 mM). Jing et al. Jing et al. (2025) pointed out that under 150 mM NaCl treatment, the growth of wild-type apple calli was significantly inhibited and the fresh weight was significantly reduced compared with *MdSPL13B-OE* apple calli. The results of this experiment showed that under 200 mM NaCl stress, the fresh weight of *A. camelorum* calli decreased by 15.8% after 14 days and showed slight browning, which is consistent with previous research results.

Previous studies believed that ROS are harmful to plant growth and development, so plants have evolved various strategies to alleviate oxidative stress (Ding et al. 2015), such as the antioxidant enzyme system that can scavenge or reduce ROS produced by abiotic stress and reduce cell damage. However, with in-depth research on ROS, it has been found that ROS actually play a complex dual role. Plants can use potentially toxic ROS molecules as beneficial signals for development to precisely and temporally inhibit premature maturation of the shoot apical meristem and ensure orderly flowering (Huang et al. 2021). ROS signals produced in callus cells also play an important regulatory role in the embryogenic capacity of calli (Zhou et al. 2016). Histochemical staining showed that in the absence of stress, ROS produced by *A. camelorum* calli mainly accumulated on the side in contact with the medium, with a small amount on the upper surface. This may be because changes in cell volume and number of calli are easily restricted by the cell wall, and the production of ROS signals can break down the cell wall, promote cell wall loosening, and thereby regulate cell growth (Zhang et al. 2024). However, under long-term high-concentration salt stress, calli are in a state of oxidative stress for a long time, the scavenging efficiency of the antioxidant enzyme system decreases, and high ROS levels cause damage to calli, which is not conducive to embryonic development (Ren et al. 2022), leading to browning and death.

Under NaCl stress, the activities of SOD, POD, CAT, as well as the content of MDA, all increased significantly. In the early stage of stress, the antioxidant enzyme system of *A. camelorum* calli was activated immediately. Compared with POD and CAT, SOD was activated more rapidly and catalyzed the dismutation of $O_2^{-}\bullet$ into O_2 and H_2O_2 through redox reactions. CAT has high specificity and fast turnover rate for H_2O_2 (Zhang et al. 2016), while POD uses H_2O_2 as an oxidant to catalyze various substrates such as phenols and lipid peroxides, and the two synergistically scavenge the produced H_2O_2.

In the late stage of stress, MDA content continued to increase, SOD activity decreased to the initial stress level, CAT activity decreased significantly, while POD always maintained high activity. This may be because long-term stress provided more substrates such as phenols for POD, so POD played a major role in the late stage of stress and undertook important antioxidant or secondary metabolic regulatory functions. The decrease in SOD and CAT activities may be related to the consumption of the enzyme

system caused by continuous stress. H_2O_2, as a signaling molecule, can induce CAT to initiate defense responses, while excessive ROS can cause oxidative damage to calli, resulting in fluctuating CAT activity.

Plants can maintain the active function of SOD and POD for a longer period than CAT when facing stress, and SOD and POD show better synergy (Zhang et al. 2006). Long-term stress leads to the decline of antioxidant system function, and the activities of SOD and POD show a trend of first increasing and then decreasing (Zhang et al. 2025), which is similar to the results of this experiment. In conclusion, the three key protective enzymes regulated by the antioxidant enzyme system of *A. camelorum* calli maintain the normal level of ROS in the body through coordinated interaction, reducing ROS damage to calli.

Based on the research results of (Tang et al. 2024), we screened Asp07G015930, which showed the highest upregulation of gene expression in *A. camelorum* calli under salt stress, from 10 candidate genes. The CDS length of this gene is 1080 bp, encoding 359 amino acids. Bioinformatics analysis showed that the protein encoded by this gene is hydrophilic, has no signal peptide, is mainly composed of helix structures, has high homology with ABI5 proteins in various plants, and has conserved functional domains typical of the bZIP family.

Abscisic acid (ABA) is involved in regulating signal transduction in various defense processes to resist abiotic and biotic stresses and promote plant development (Sah et al. 2016). The bZIP family is divided into 13 major groups, among which Group A mainly consists of ABA-responsive element-binding protein (AREB), ABA-responsive element-binding factor (ABF), and ABI5 subfamily members (Collin et al. 2021). As a core protein in the ABA signal transduction pathway, ABI5 plays an important regulatory role in seed germination, early seedling development, and stress adaptation. Research findings indicate that numerous ABA-insensitive (*ABI*) genes exist in *Arabidopsis thaliana*, including *ABI1*, *ABI2*, *ABI3*, *ABI4*, and *ABI5*. Among them, ABI1 and ABI2 are two highly homologous protein kinases that act as negative regulators in the ABA signaling pathway (Merlot et al. 2001); ABI3 belongs to the B3 protein family (Xu et al. 2022) and plays a key role in regulating plant flowering; ABI4 belongs to the CBF/DREB subfamily, is a member of the AP2/ERF family, contains an AP2 domain, and is involved in ABA signal transduction (Yang 2025); ABI5 belongs to the bZIP transcription factor and is a core transcription factor in the ABA signal transduction pathway (Du et al. 2025; Du et al. 2024). Based on its function and sequence characteristics, the gene was named *AcABI5*. Zinsmeister et al. confirmed the role of ABI5 in regulating ROS accumulation and seed maturation in Pisum sativum, a leguminous plant ; Finkelstein et al. found that ABI5 regulates the expression of downstream genes such as late embryogenesis abundant (LEA) proteins, and is involved in processes including seed germination and dehydration tolerance (Zinsmeister et al. 2016); Albertos et al. revealed that nitric oxide can counteract ABA during plant development and regulate the molecular interaction mechanism of ABI5 through post-translational modification (Albertos et al. 2015); Basso et al. (2025) comprehensively analyzed the *AREB/ABF/ABI5* genes belonging to the subfamily A of plant bZIP TFs in *C. arietinum* and *Lens culinaris*, which are up-regulated under different abiotic and biotic stress conditions, exhibit dynamic expression in different tissues, and show higher expression levels in drought-tolerant varieties. We speculate that AcABI5 has similar functions to these homologous proteins, possibly binding to cis-acting elements to regulate the

transcriptional expression of downstream genes, and playing a key role in plant responses to abiotic stress and seed germination. Most studies have shown that typical TFs are usually localized in the nucleus of plant cells (Wang et al. 2021). By constructing the pK7WGF2-35S::GFP-AcABI5 fusion expression vector and using *Agrobacterium* to infect *N. benthamiana* leaves for transient expression, the results showed that the fusion protein emitted fluorescence only in the nucleus, indicating that AcABI5, like most TFs, is a nuclear-localized protein. Through salt stress treatment of *A. camelorum* calli, we found that *AcABI5* can respond rapidly to salt stress and maintain high expression during the stress process; in the absence of abiotic stress, ABI5 undergoes dephosphorylation, and the dephosphorylated ABI5 is neither active nor stable and will be degraded through the 26S proteasome pathway (Lopez-Molina et al. 2001), which is consistent with the low expression level of *AcABI5* observed in our control group. In future research, we will further establish an *AcABI5* overexpression system in *A. camelorum* calli, identify the cis-acting elements bound by AcABI5, analyze the downstream target genes regulated by AcABI5, and investigate whether AcABI5 regulates the expression of salt resistance-related genes by binding to these cis-acting elements.

Conclusions

This study determined that the optimal proliferation medium for *A. camelorum* calli is 1.5 mg/L 2,4-D combined with 0.5 mg/L 6-BA. In response to salt stress, SOD in *A. camelorum* calli is activated first to scavenge intracellular O_2^-•; POD and CAT synergistically scavenge ROS in the early stage of stress, and POD also exhibits high activity in the late stage of stress. A salt-tolerant gene *AcABI5* of *A. camelorum* was screened out by qRT-PCR, with a full-length CDS sequence of 1080 bp encoding 359 amino acids. Bioinformatics analysis revealed that AcABI5 from *A. camelorum* is a nuclear-localized bZIP family TF with typical conserved domains; its promoter region contains stress-responsive cis-acting elements. This TF harbors conserved transcriptional regulatory functions, and the gene is inducible in *A. camelorum* calli under salt stress, suggesting that AcABI5 may be involved in the regulatory network of *A. camelorum* adapting to abiotic stresses including drought and salt stress. This study provides a research basis for further investigating the molecular mechanism of *AcABI5* regulating *A. camelorum*'s response to salt stress, and offers theoretical support for the establishment of a genetic transformation system for *A. camelorum*.

Declarations

Data Availability

Data of this study will be made available on reasonable request.

Funding

This research was funded by the Key Laboratory of Ecological Safety and Sustainable Development in Arid Lands Young Scientists Interdisciplinary Team Project (grant No.E552020301), the National Key

Research and Development Program of China (grant No.2022YFF1302505-03), and the National Young Talent Program (grant No.2022000007).

Competing Interests

The authors have no competing interests to declare that are relevant to the content of this article.

Ethics Approval

Not applicable.

Author Contributions

All authors contributed to the study conception and design. Material preparation, data collection and analysis were performed by, Xiangyi Li, Pingyin Guan, Bo Zhang and Gangliang Tang. The first draft of the manuscript was written by Zhengtao Yan and all authors commented on previous versions of the manuscript. All authors read and approved the final manuscript.

References

1. Albertos P, Romero-Puertas MC, Tatematsu K, Mateos I, Sánchez-Vicente I, Nambara E, Lorenzo O (2015) S-nitrosylation triggers ABI5 degradation to promote seed germination and seedling growth. Nat Commun 6:8669. https://doi.org/10.1038/ncomms9669
2. Basso MF, Iovieno P, Capuana M, Contaldi F, Ieri F, Menicucci F, Celso FL, Barone G, Martinelli F (2025) Identification and expression of the AREB/ABF/ABI5 subfamily genes in chickpea and lentil reveal major players involved in ABA-mediated defense response to drought stress. Planta 262(1):22. https://doi.org/10.1007/s00425-025-04740-y
3. Bu H, Jia J, Hao J (2000) Establishment of a high efficient regeneration system in Alhagi pseudalhagi. Journal of Northwest University(Natural Science Edition)(06):505-508+548. https://doi.org/10.16152/j.cnki.xdxbzr.2000.06.014
4. Chai M, Yang F, Cai S, Liu T, Xu X, Huang Y, Xi X, Yang J, Cao Z, Sun L, Dou D, Fang X, Yan M, Cai H (2025) Overexpression of the Transcription Factor GmbZIP60 Increases Salt and Drought Tolerance in Soybean (Glycine max). Int J Mol Sci 26(7). https://doi.org/10.3390/ijms26073455
5. Chen C, Wu Y, Li J, Wang X, Zeng Z, Xu J, Liu Y, Feng J, Chen H, He Y, Xia R (2023) TBtools-II: A "one for all, all for one" bioinformatics platform for biological big-data mining. Mol Plant 16(11):1733-1742. https://doi.org/10.1016/j.molp.2023.09.010
6. Collin A, Daszkowska-Golec A, Szarejko I (2021) Updates on the Role of ABSCISIC ACID INSENSITIVE 5 (ABI5) and ABSCISIC ACID-RESPONSIVE ELEMENT BINDING FACTORs (ABFs) in ABA Signaling in Different Developmental Stages in Plants. Cells 10(8). https://doi.org/10.3390/cells10081996

7. Ding ZJ, Yan JY, Li CX, Li GX, Wu YR, Zheng SJ (2015) Transcription factor WRKY46 modulates the development of Arabidopsis lateral roots in osmotic/salt stress conditions via regulation of ABA signaling and auxin homeostasis. The Plant Journal 84(1):56-69. https://doi.org/10.1111/tpj.12958
8. Dong Z, Zhang S (2000) The Resources and Utilization of Alhagi maurorum in Arid and Desert Zone. Grassland of China(04):74-76(in chinese).
9. Du C, Bai H, Yan Y, Liu Y, Wang X, Zhang Z (2025) Exploring ABI5 regulation: Post-translational control and cofactor interactions in ABA signaling. Plant J 121(3):e17232. https://doi.org/10.1111/tpj.1723210.1111/tpj.17232
10. Du C, Liu M, Yan Y, Guo X, Cao X, Jiao Y, Zheng J, Ma Y, Xie Y, Li H, Yang C, Gao C, Zhao Q, Zhang Z (2024) The U-box E3 ubiquitin ligase PUB35 negatively regulates ABA signaling through AFP1-mediated degradation of ABI5. Plant Cell 36(9):3277-3297. https://doi.org/10.1093/plcell/koae194
11. Hassanein AM (2004) Hormonal Requirements Induced Different Regeneration Pathways in Alhagi graecorum. Journal of Plant Biotechnology.
12. He Q, Cai H, Bai M, Zhang M, Chen F, Huang Y, Priyadarshani S, Chai M, Liu L, Liu Y, Chen H, Qin Y (2020) A Soybean bZIP Transcription Factor GmbZIP19 Confers Multiple Biotic and Abiotic Stress Responses in Plant. Int J Mol Sci 21(13). https://doi.org/10.3390/ijms21134701
13. Hossain MA, Bhattacharjee S, Armin SM, Qian P, Xin W, Li HY, Burritt DJ, Fujita M, Tran LS (2015) Hydrogen peroxide priming modulates abiotic oxidative stress tolerance: insights from ROS detoxification and scavenging. Front Plant Sci 6:420. https://doi.org/10.3389/fpls.2015.00420
14. Huang X, Chen S, Li W, Tang L, Zhang Y, Yang N, Zou Y, Zhai X, Xiao N, Liu W, Li P, Xu C (2021) ROS regulated reversible protein phase separation synchronizes plant flowering. Nature Chemical Biology 17(5):549-557. https://doi.org/10.1038/s41589-021-00739-0
15. Jing X, Wang D, Liu X, Chen G, Guo X, Wang X-F, Zhang Z, You C-X (2025) The SBP transcription factor MdSPL13B positively regulates salt tolerance in apple. Horticultural Plant Journal. https://doi.org/10.1016/j.hpj.2025.01.008
16. Juan CA, Pérez de la Lastra JM, Plou FJ, Pérez-Lebeña E (2021) The Chemistry of Reactive Oxygen Species (ROS) Revisited: Outlining Their Role in Biological Macromolecules (DNA, Lipids and Proteins) and Induced Pathologies. Int J Mol Sci 22(9). https://doi.org/10.3390/ijms22094642
17. Kazemi M, Ghasemi Bezdi K (2021) An investigation of the nutritional value of camelthorn (Alhagi maurorum) at three growth stages and its substitution with part of the forage in Afshari ewes' diets. Animal Feed Science and Technology 271:114762. https://doi.org/10.1016/j.anifeedsci.2020.114762
18. Livak KJ, Schmittgen TD (2001) Analysis of Relative Gene Expression Data Using Real-Time Quantitative PCR and the $2^{-\Delta\Delta CT}$ Method. Methods 25(4):402-408. https://doi.org/10.1006/meth.2001.1262
19. Lopez-Molina L, Mongrand S, Chua NH (2001) A postgermination developmental arrest checkpoint is mediated by abscisic acid and requires the ABI5 transcription factor in Arabidopsis. Proceedings

of the National Academy of Sciences of the United States of America 98(8):4782-7. https://doi.org/10.1073/pnas.081594298

20. Manafu Z, Zhang Z, Malajiang X, Abula S, Guo Q, Wu Y, Wusiman A, Bake B (2024) Effects of Alhagi camelorum Fisch polysaccharide from different regions on growth performance and gastrointestinal microbiota of sheep lambs. Frontiers in Pharmacology Volume 15 - 2024. https://doi.org/10.3389/fphar.2024.1379394
21. Merlot S, Gosti F, Guerrier D, Vavasseur A, Giraudat J (2001) The ABI1 and ABI2 protein phosphatases 2C act in a negative feedback regulatory loop of the abscisic acid signalling pathway. Plant J 25(3):295-303. https://doi.org/10.1046/j.1365-313x.2001.00965.x
22. Muhammad G, Hussain MA, Anwar F, Ashraf M, Gilani AH (2014) A Plant Genus Rich in Bioactives for Pharmaceuticals. Birkhäuser Boston. https://doi.org/1007/978-0-8176-4697-4_3.
23. Muhammad G, Hussain MA, Anwar F, Ashraf M, Gilani AH (2015) Alhagi: A Plant Genus Rich in Bioactives for Pharmaceuticals. Phytotherapy Research 29.
24. Murashige T, Skoog F (1962) A Revised Medium for Rapid Growth and Bio Assays with Tobacco Tissue Cultures. Physiologia Plantarum 15(3):473-497. https://doi.org/10.1111/j.1399-3054.1962.tb08052.x
25. Pirasteh-Anosheh H, Parvizi H, Parnian A, Esfahan EZ, Ranjbar G, Bhardwaj AK (2022) Relationship between soil salinity and alkalinity with Alhagi camelorum growth in hypersaline and hyperarid environments. Journal of Arid Environments 206:104830. https://doi.org/10.1016/j.jaridenv.2022.104830
26. Ren N, Zou M, Chen G, Shen X (2022) Difference Analysis of Redox Levels in the Callus of *Agapanthus praecox* ssp. *orientalis* with Different Embryogenic Ability. Molecular Plant Breeding 20(04):1281-1288(in Chinese). https://doi.org/10.13271/j.mpb.020.001281
27. Sah SK, Reddy KR, Li J (2016) Abscisic Acid and Abiotic Stress Tolerance in Crop Plants. Front Plant Sci 7:571. https://doi.org/10.3389/fpls.2016.00571
28. Song L (2019) Studies on the effects of epibrassinolide on eallus erowtth
29. and regeneration of *Zoysia matrella* (L.) Merr. under Salt Stress. Dissertation, Zhejiang University,China(in Chinese)
30. Srivastava B, Sharma H, Dey YN, Wanjari MM, Jadhav AD (2014) Alhagi pseudalhagi: a review of its phyto-chemistry, pharmacology, folklore claims and Ayurvedic studies. International Journal of Herbal Medicine 2:47-51.
31. Tang G, Li X, Lin L, Li L, Lu J (2013) Effects of short-term phloem girdling on physiology in two desert plants in the southern edge of the Taklimakan Desert. Chinese Journal of Plant Ecology 37(12):1101-1113(in Chinese).
32. Tang G, Li X, Zeng F, Ma J, Guan P, Zhang B (2024) Exploring the Genetic Basis of Drought Tolerance in Alhagi camelorum: A Comprehensive Transcriptome Study of Osmotic Stress Adaptations. International Journal of Molecular Sciences 25(23):12725. https://doi.org/10.3390/ijms252312725

33. Ullah A, Tariq A, Sardans J, Peñuelas J, Zeng F, Graciano C, Asghar MA, Raza A, Xiong YC, Chai X, Zhang Z (2022) Alhagi sparsifolia acclimatizes to saline stress by regulating its osmotic, antioxidant, and nitrogen assimilation potential. BMC Plant Biol 22(1):453. https://doi.org/10.1186/s12870-022-03832-1
34. van Zelm E, Zhang Y, Testerink C (2020) Salt Tolerance Mechanisms of Plants. Annu Rev Plant Biol 71:403-433. https://doi.org/10.1146/annurev-arplant-050718-100005
35. Wang R, Wang R, Liu M, Yuan W, Zhao Z, Liu X, Peng Y, Yang X, Sun Y, Tang W (2021) Nucleocytoplasmic trafficking and turnover mechanisms of BRASSINAZOLE RESISTANT1 in Arabidopsis thaliana. Proc Natl Acad Sci U S A 118(33). https://doi.org/10.1073/pnas.2101838118
36. Xu G, Tao Z, He Y (2022) Embryonic reactivation of FLOWERING LOCUS C by ABSCISIC ACID-INSENSITIVE 3 establishes the vernalization requirement in each Arabidopsis generation. Plant Cell 34(6):2205-2221. https://doi.org/10.1093/plcell/koac077
37. Xu Z, Ali Z, Xu L, He X, Huang Y, Yi J, Shao H, Ma H, Zhang D (2016) The nuclear protein GmbZIP110 has transcription activation activity and plays important roles in the response to salinity stress in soybean. Sci Rep 6:20366. https://doi.org/10.1038/srep20366
38. Yang L (2025) Arabidopsis ABFs and ABI4 Cooperatively Regulate Primary Root Growth in Response to ABA. Dissertation, Shandong Agricultural University,China(in Chinese)
39. Yue L, Pei X, Kong F, Zhao L, Lin X (2023) Divergence of functions and expression patterns of soybean bZIP transcription factors. Front Plant Sci 14:1150363. https://doi.org/10.3389/fpls.2023.1150363
40. Zeng F, Zhang X, Li X (2002) study on the characteristics of alhagi and its impact on resource protection and development. Arid Land Geography(03):286-288(in Chinese). https://doi.org/10.13826/j.cnki.cn65-1103/x.2002.03.019
41. Zhang L, Han S, Li Z, Liu N, Li L, Luo L, Peng T, Liu W (2006) Effects of *Actinote thalia pyrrha* (Fabricius) feeding on the physiological indexes in *Mikania micrantha* leaves. Acta Ecologica Sinica(05):1330-1336(in Chinese).
42. Zhang N, Kuang L, Yang L, Wang Y, Han F, Zhang Y, Wang S, Lv H, Ji J (2025) Integrated Transcriptomics and Metabolomics Analysis Reveals Convergent and Divergent Key Molecular Networks of Dominant Genic Male Sterility and Cytoplasmic Male Sterility in Cabbage. Int J Mol Sci 26(3). https://doi.org/10.3390/ijms26031259
43. Zhang Y, Cai G, Zhang K, Sun H, Huang L, Ren W, Ding Y, Wang N (2024) PdeERF114 recruits PdeWRKY75 to regulate callus formation in poplar by modulating the accumulation of H_2O_2 and the relaxation of cell walls. New Phytologist 241(2):732-746. https://doi.org/10.1111/nph.19349
44. Zhang Z, Xu Y, Xie Z, Li X, He Z-H, Peng X-X (2016) Association–Dissociation of Glycolate Oxidase with Catalase in Rice: A Potential Switch to Modulate Intracellular H_2O_2 Levels. Molecular Plant 9(5):737-748. https://doi.org/10.1016/j.molp.2016.02.002
45. Zheng Y, Cao X, Zhou Y, Li Z, Yang Y, Zhao D, Li Y, Xu Z, Zhang C-S (2023) Effect of planting salt-tolerant legumes on coastal saline soil nutrient availability and microbial communities. Journal of

Environmental Management 345:118574. https://doi.org/10.1016/j.jenvman.2023.118574

46. Zhou T, Yang X, Guo K, Deng J, Xu J, Gao W, Lindsey K, Zhang X (2016) ROS Homeostasis Regulates Somatic Embryogenesis via the Regulation of Auxin Signaling in Cotton. Mol Cell Proteomics 15(6):2108-24. https://doi.org/10.1074/mcp.M115.049338
47. Zinsmeister J, Lalanne D, Terrasson E, Chatelain E, Vandecasteele C, Vu BL, Dubois-Laurent C, Geoffriau E, Signor CL, Dalmais M, Gutbrod K, Dörmann P, Gallardo K, Bendahmane A, Buitink J, Leprince O (2016) ABI5 Is a Regulator of Seed Maturation and Longevity in Legumes. Plant Cell 28(11):2735-2754. https://doi.org/10.1105/tpc.16.00470

Figures

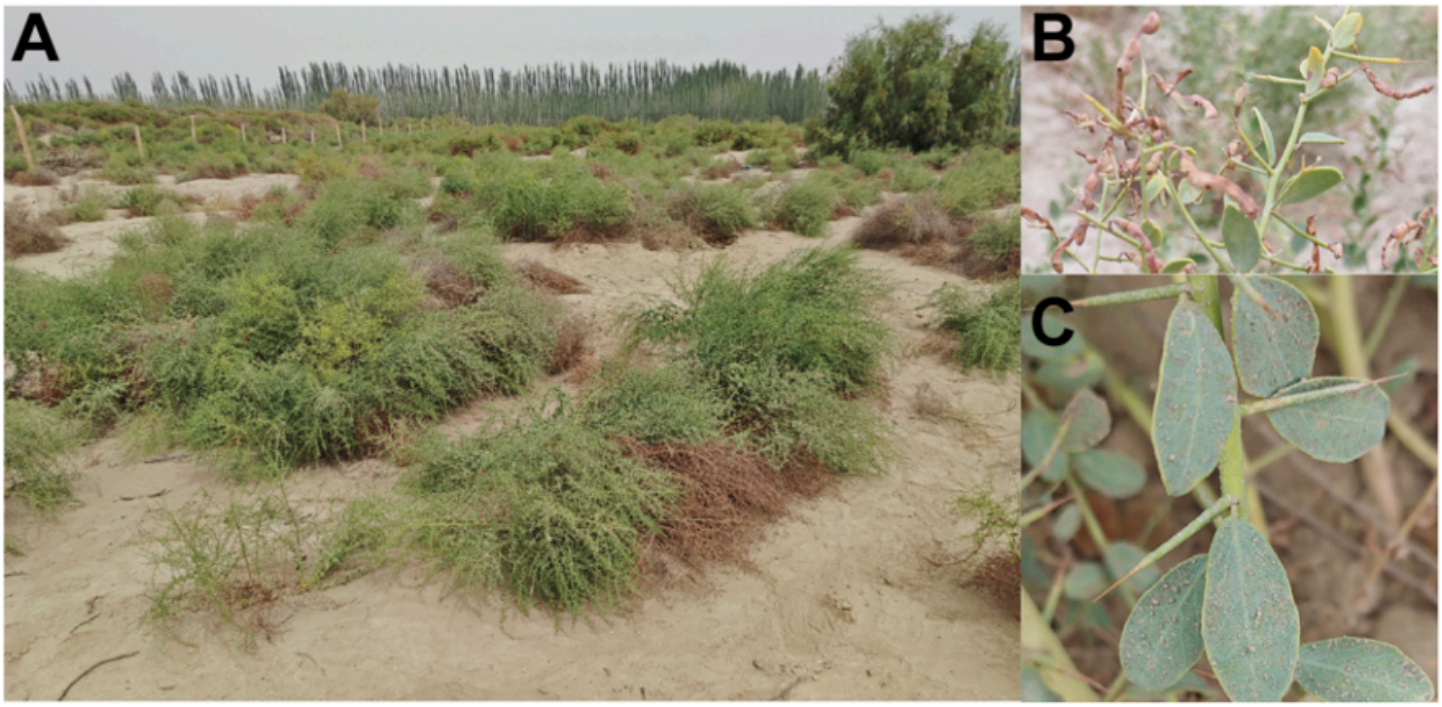


Figure 1

(A) *A. camelorum*thrives in arid and saline-alkali habitat. (B) The fruit of *A. camelorum.*(C) Leaves and thorns of *A. camelorum*. The images were taken in the southern margin of the Taklamakan Desert

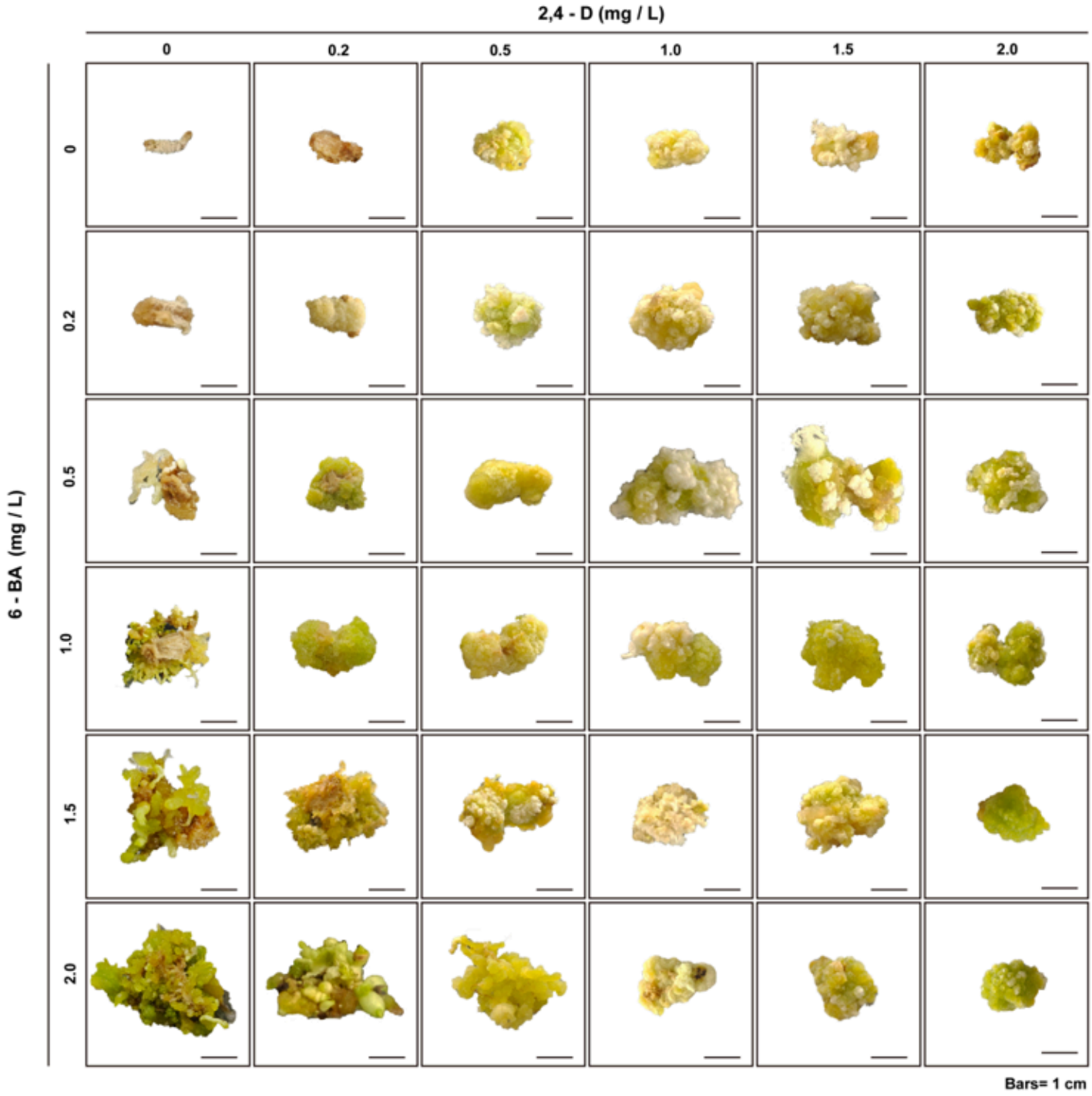


Figure 2

Effects of different hormone concentrations on callus induction.The abscissa represents the concentration of 2,4-D (0–2 mg/L), the ordinate represents the concentration of 6-BA (0–2 mg/L), and each grid corresponds to one type of hormone combination. Bar = 1 cm

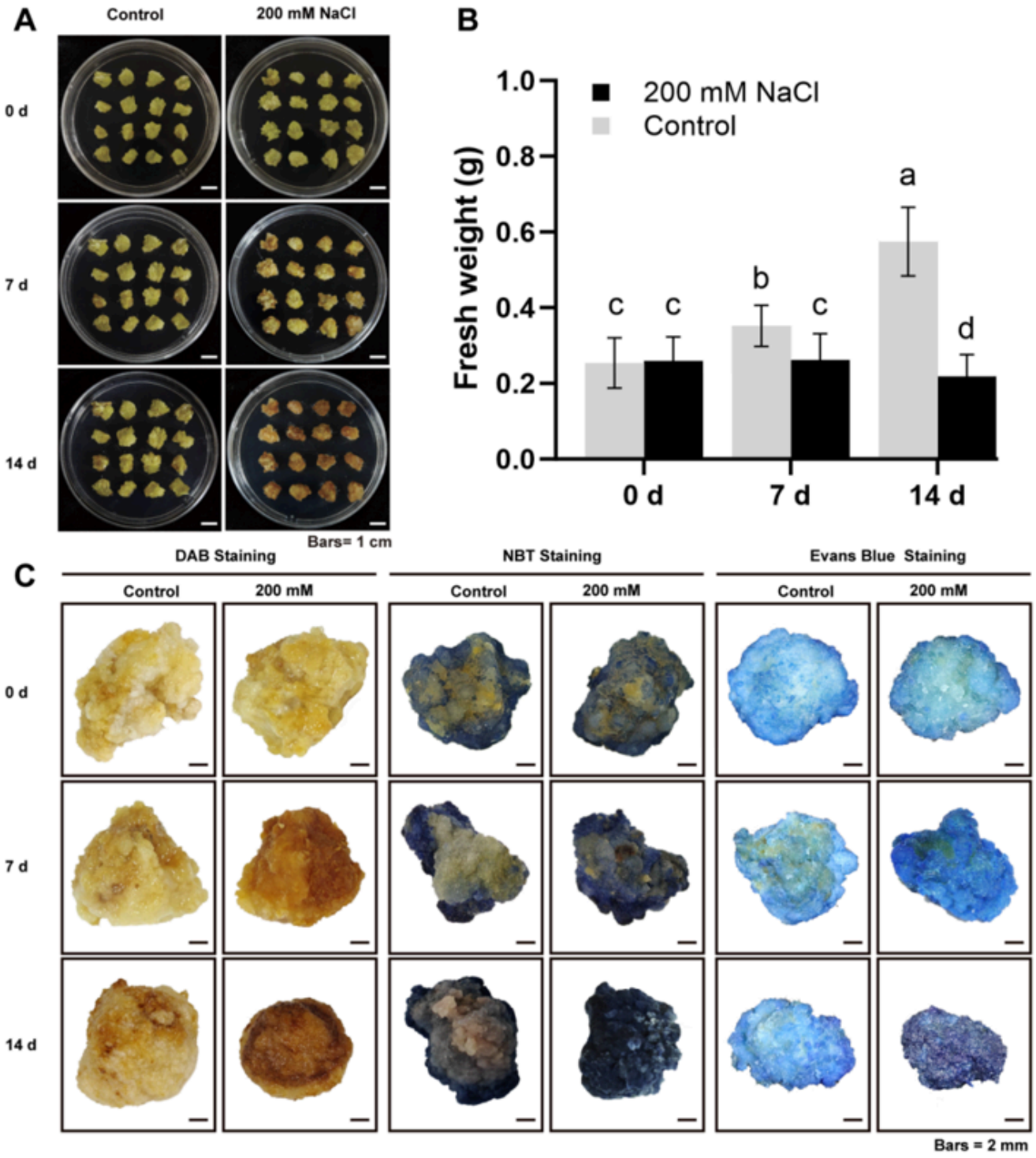


Figure 3

(A) Phenotypic changes (Bar = 1 cm) and (B) fresh weight changes of calli under salt stress. (C) DAB, NBT and Evans Blue Staining of *A. camelorum* calli (Bar = 2 mm). Different lowercase letters indicate significant differences according to the Duncan's test ($P < 0.05$). Data are presented as the mean ± SD ($n = 3$ independent biological replicates)

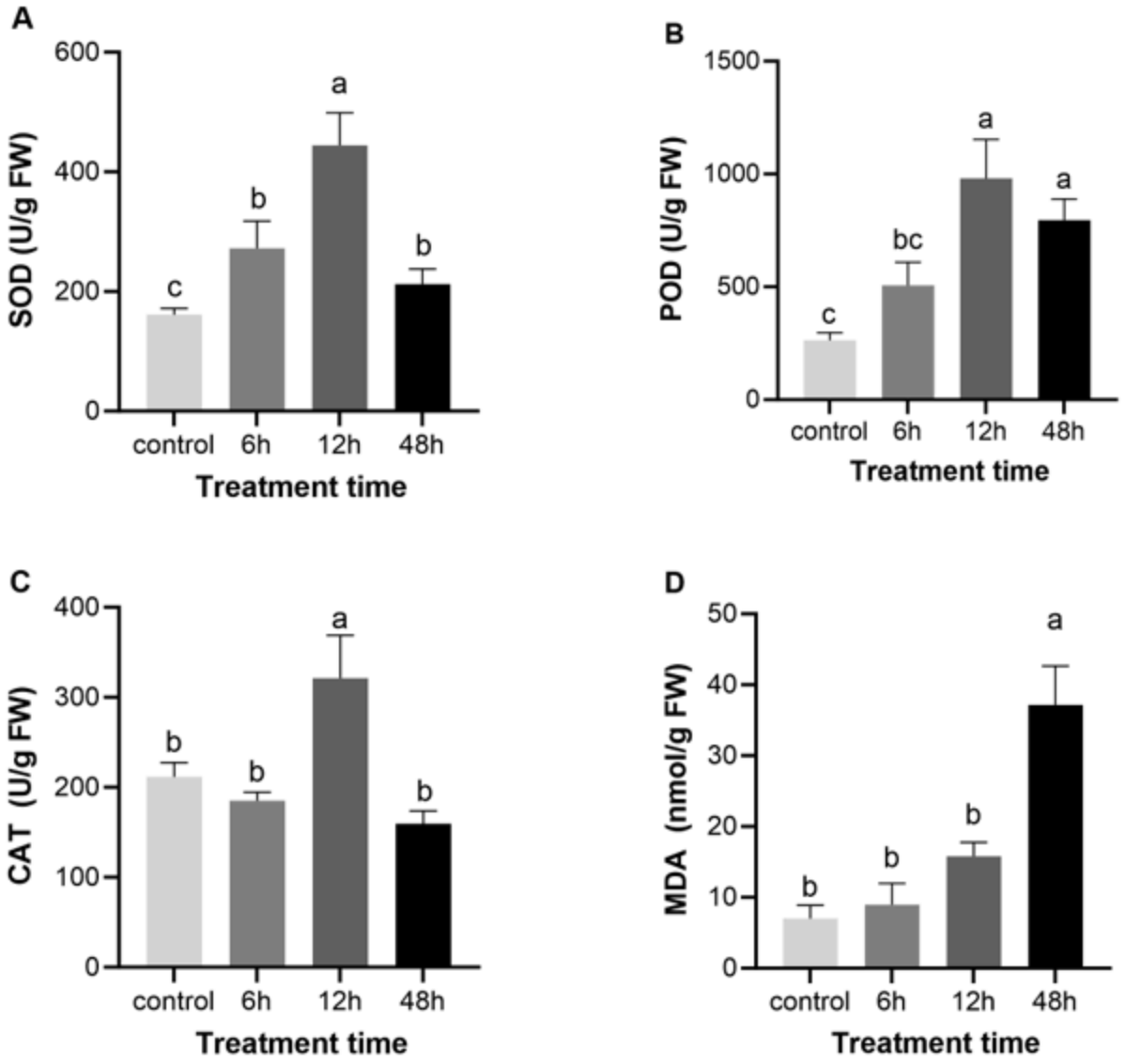


Figure 4

Determination of (A) SOD,(B) POD and (C) CAT activities as well as (D) MDA content. Different lowercase letters indicate significant differences according to the Duncan's test ($P < 0.05$). Data are presented as the mean ± SD ($n = 3$ independent biological replicates)

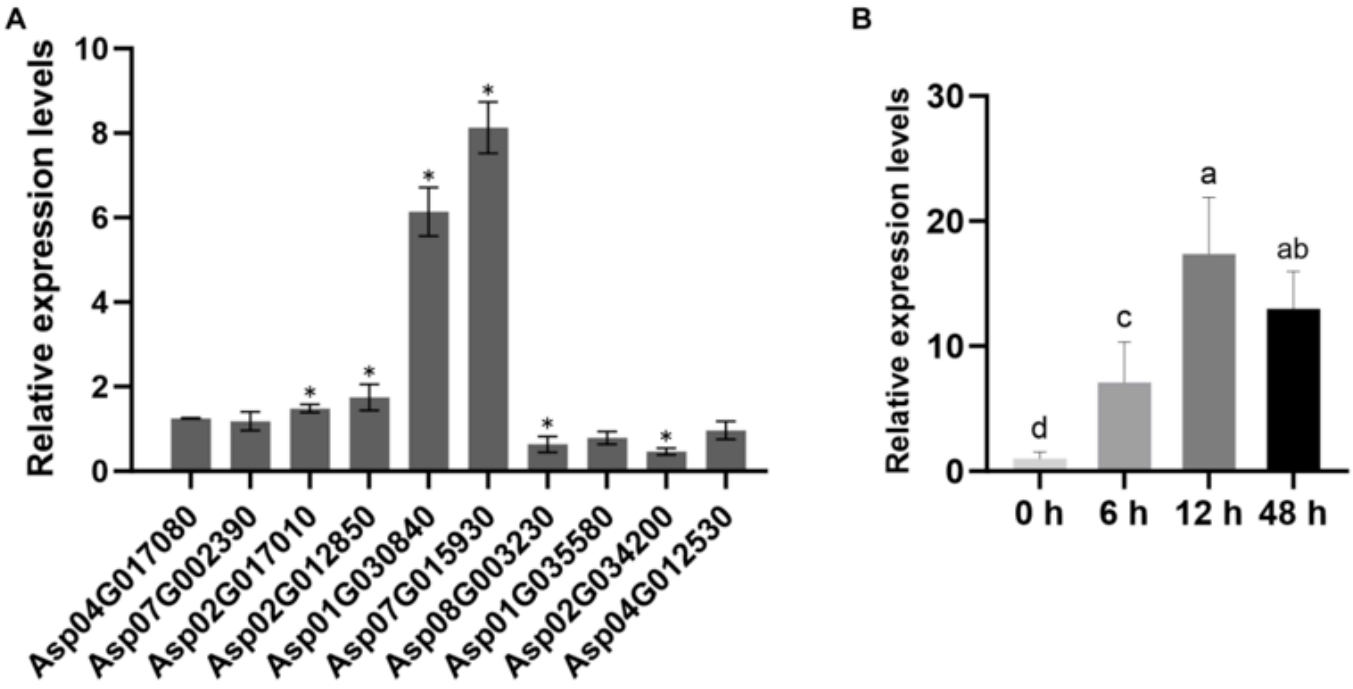


Figure 5

(A) Relative expression levels of different genes in callus. Each gene was individually analyzed using Student's t-test, asterisks indicate significant differences compared to the control group ($P < 0.05$) (B) Relative expression level of *AcABI5* in callus at different time points. Different lowercase letters indicate significant differences according to the Duncan's test ($P < 0.05$). Data are presented as the mean ± SD ($n = 3$ independent biological replicates)

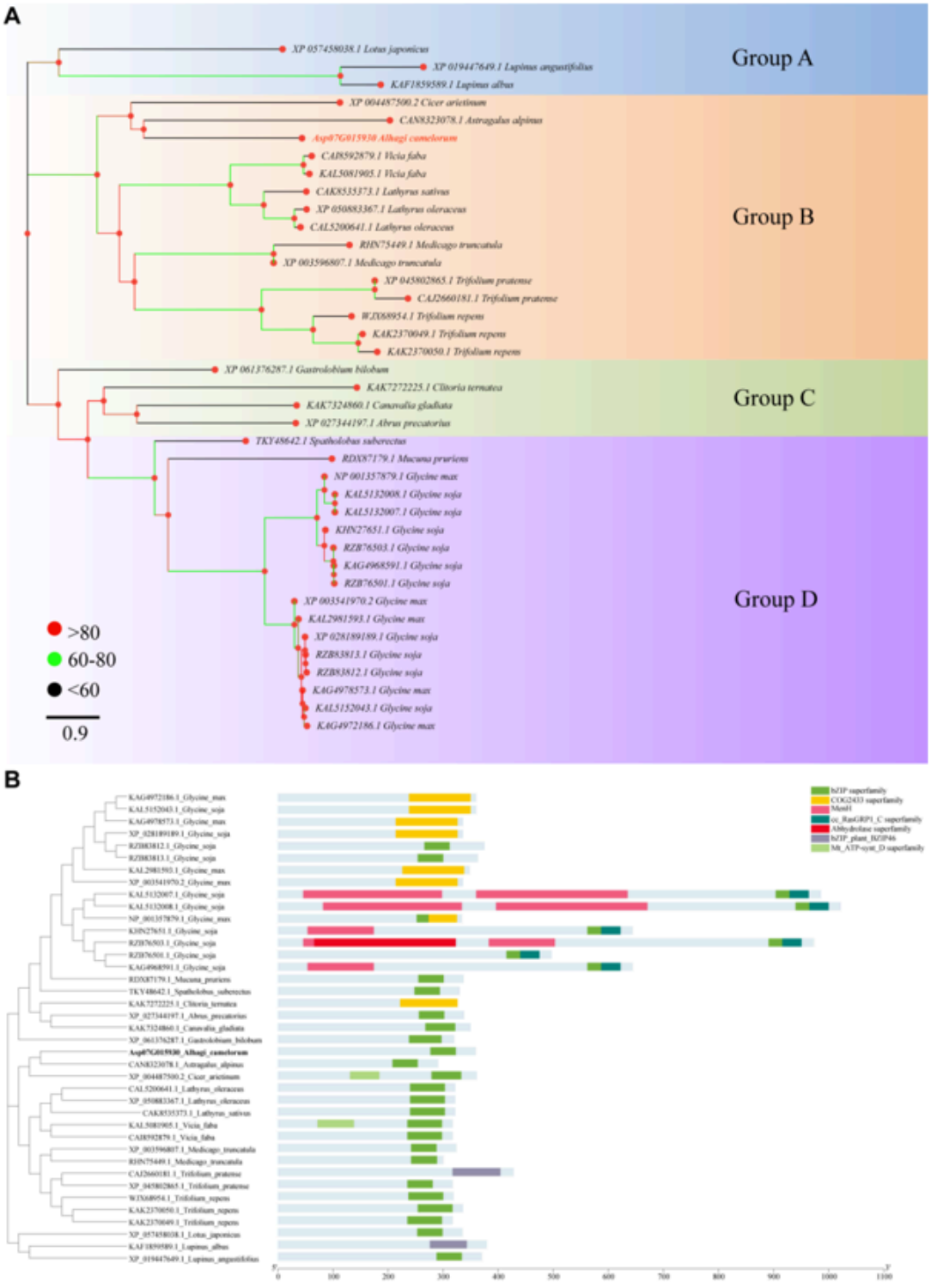


Figure 6

(A) Phylogenetic tree constructed based on ABI5 homologous proteins identified from *A. camelorum*, *M. truncatula* , *C. arietinum* and other plants. (B) Conserved domain and motif analysis was performed on ABI5 homologous proteins identified from *A. camelorum*,*M. truncatula*, *C. arietinum* and other plants

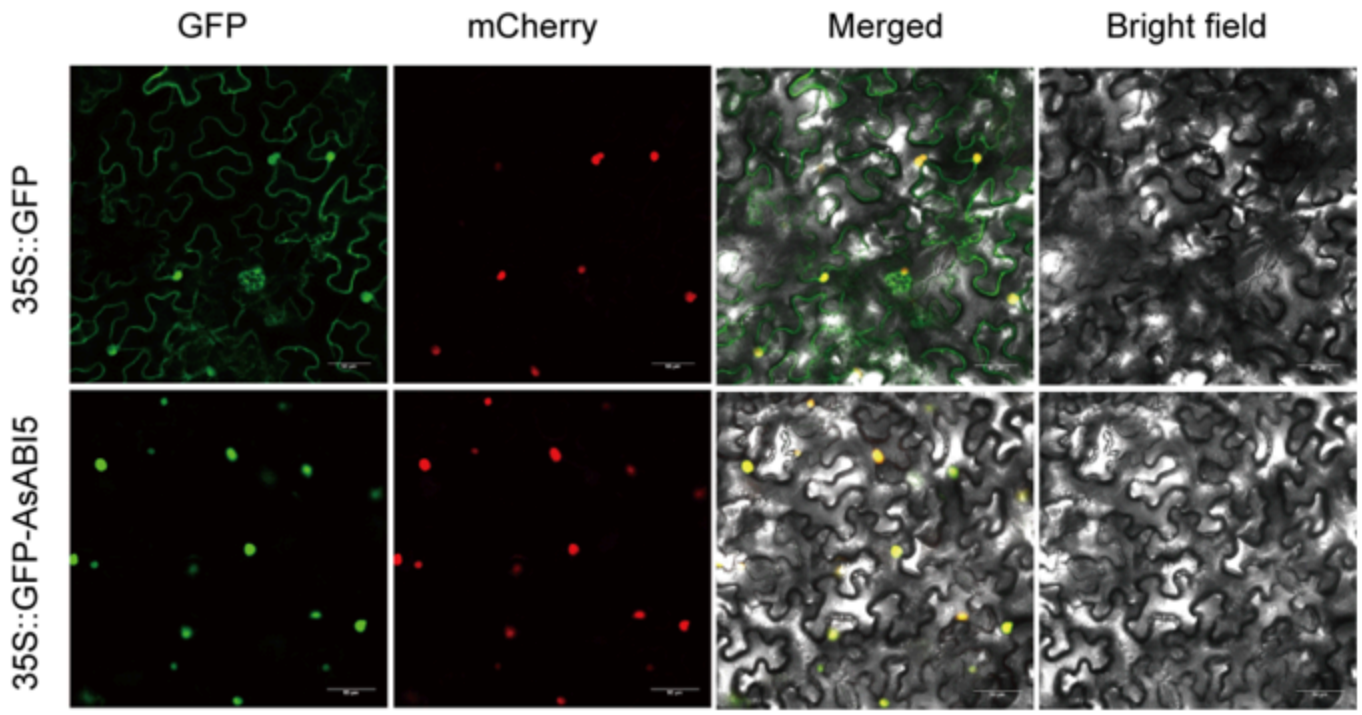


Figure 7

Subcellular localization of AcABI5 in *N. benthamiana* leaves. The signals from GFP fluorescence, mCherry, merged, and bright field images are shown.EGFP: excitation at 488 nm, emission at 507 nm; mCherry: excitation at 587 nm, emission at 610 nm (Bar = 50 μm)